HHS Public Access

Author manuscript

Biol Psychiatry. Author manuscript; available in PMC 2022 April 15.

Published in final edited form as:

Biol Psychiatry. 2021 April 15; 89(8): 795–806. doi:10.1016/j.biopsych.2020.06.010.

Aging-sensitive networks within the human structural connectome are implicated in late-life cognitive declines

James W. Madole[1,*,†], **Stuart J. Ritchie**[2,†], **Simon R. Cox**[3,4,5], **Colin R. Buchanan**[3,4,5], **Maria Valdés Hernández**[3,5,6], **Susana Muñoz Maniega**[3,5,6], **Joanna M. Wardlaw**[3,5,6], **Mat A. Harris**[7], **Mark E. Bastin**[3,5,6], **Ian J. Deary**[3,4], **Elliot M. Tucker-Drob**[1,8]

[1]Department of Psychology, University of Texas at Austin, Austin, TX

[2]Social, Genetic and Developmental Psychiatry Centre, King's College London, London, UK

[3]Lothian Birth Cohorts, University of Edinburgh, Edinburgh, UK

[4]Department of Psychology, University of Edinburgh, Edinburgh, UK

[5]Scottish Imaging Network, A Platform for Scientific Excellence (SINAPSE) Collaboration, Edinburgh, UK

[6]Centre for Clinical Brain Sciences, University of Edinburgh, Edinburgh, UK

[7]Division of Psychiatry, University of Edinburgh, Edinburgh, UK

[8]Population Research Center, University of Texas at Austin, Austin, TX

Abstract

Background—Aging-related cognitive decline is a primary risk factor for Alzheimer's disease and related dementias. More precise identification of the neurobiological bases of cognitive decline in aging populations may provide critical insights into the precursors of late-life dementias.

Methods—Using structural and diffusion brain MRI data from the UK Biobank (UKB; N = 8,185, ages 45–78 years), we examined aging of regional grey matter volumes (*nodes*) and white matter structural connectivity (*edges*) within nine well-characterized networks-of-interest in the

[*]Correspondence to: James W. Madole, M.A., Department of Psychology, The University of Texas at Austin, 108 E. Dean Keeton Street, Stop A8000, Austin, TX 78712, USA. jmadole@utexas.edu.

Author contributions

SJR, EMT-D, & JWM conceived of the study design. CRB & SRC processed the UKB MRI data. SRC, MAH, & MVH processed the LBC1936 MRI data. JWM and SJR conducted the analyses under supervision from EMT-D. JWM, SJR & EMT-D wrote the paper. All authors contributed edits and feedback on the paper.

[†]These authors contributed equally to this work

Conflicts of interest

Authors JWM, SJR, SRC, CRB, MVH, SMM, JMW, MAH, MEB, & EMT-D have no biomedical financial interests or potential conflicts of interest. Author IJD is a participant in UK Biobank.

Data availability

UKB-derived age- and PC-weights for connectome elements are available as Table S10.

human brain connectome. In the independent Lothian Birth Cohort 1936 (LBC1936; $N = 534$, all age 73 years), we tested whether aging-sensitive connectome elements are enriched for key domains of cognitive function, before and after controlling for early-life cognitive ability.

Results—In UKB, age-differences in individual connectome elements corresponded closely with principal component loadings reflecting connectome-wide integrity ($|r_{nodes}| = 0.420$; $|r_{edges}| = 0.583$), suggesting that connectome aging occurs on broad dimensions of variation in brain architecture. In LBC1936, composite indices of node integrity were predictive of all domains of cognitive function, whereas composite indices of edge integrity were associated specifically with processing speed. Elements within the Central Executive network were disproportionately predictive of late-life cognitive function relative to the network's small size. Associations with processing speed and visuospatial ability remained after controlling for childhood cognitive ability.

Conclusions—These results implicate global dimensions of variation in the human structural connectome in aging-related cognitive decline. The Central Executive network may demarcate a constellation of elements that are centrally important to age-related cognitive impairments.

Keywords

cognitive decline; structural MRI; diffusion MRI; connectomics; brain networks; brain age

Introduction

Non-clinical variation in cognitive decline is a primary risk factor for Alzheimer's disease and related dementias (1,2). These declines have consequences both for individuals, who may be less able to perform important everyday functions (3,4), and for aging societies, whose workforce productivity and social and medical resources may be prematurely exhausted (5). Delineating the neurodegenerative processes underlying aging-related cognitive decline may crucially advance our ability to detect, and ultimately prevent or mitigate aging-related cognitive impairments.

The human brain exhibits widespread structural changes with aging (6), the patterning of which is only partly documented (7). Measures of whole- and regional-brain volumes (8–10) and tract-level white matter microstructure (11–14) have been linked to cognitive function and age-related cognitive decline. It is not yet known which aging-related changes in brain structure underscore adult cognitive functioning. Following the best practices for predictive modeling (15,16), we take a cross-cohort magnetic resonance imaging (MRI) approach to identify elements of brain morphometry and interregional white matter connectivity that show sensitivity to aging and are relevant to late-life cognitive function.

We model each participant's brain as a macroscale *connectome*: a network of discrete grey matter regions (*nodes*) that are connected by bundles of myelinated white matter fibers (*edges*) (17). Guided by research spanning multiple brain imaging and mapping modalities (e.g., structural MRI, task-related fMRI, resting-state MRI, lesion-based mapping), we investigate nine well-characterized networks-of-interest (NOIs) within the *structural connectome* implicated in a variety of cognitive (18,19), affective (20,21), psychomotor

(22,23), and homeostatic (24,25) processes. We hypothesize that those networks previously implicated in general cognitive function (e.g., Parieto-Frontal Integration Theory (PFIT) (26,27)), will show more pronounced associations with cognitive aging than those supporting more basic functions (e.g., Sensorimotor (22,23)). These subnetworks are distributed throughout the brain and partially overlap, allowing us to examine whether age- or cognitive-relevant information is more tightly concentrated within certain heterogeneous subcomponent constellations.

Previous studies implicating the human structural connectome in age-related cognitive decline have largely documented age trends in summary indices of connectome topology (e.g., *strength*, *global efficiency*) (28,29), or have used large-scale, exploratory methods to examine how a range of morphometric and diffusion tensor measures relate to age and sociodemographic variables (30,31). In over 8,000 individuals from UK Biobank (UKB), we examine age trends for individual elements within the whole-brain connectome and its NOIs, before exploring how these age trends relate to general dimensions of neurostructural integrity. We use regression weights discovered in UKB to construct summary indices of volumetric structure and white matter connectivity at age-73 years in the independent Lothian Birth Cohort 1936 (LBC1936), which we use to predict concurrent measures of processing speed, visuospatial ability, and memory. We examine the robustness of these associations relative to controls for total brain volume (TBV) and age-11 cognitive ability.

Methods and Materials

Participants

UK Biobank.—We analyzed MRI data from 8,185 participants (4,315 female) from UK Biobank (UKB), a large-scale population epidemiology study of individuals across Great Britain (32) (see Supplementary Materials for details). Participants ranged in age from 44.64 – 78.17 years (mean = 61.9; SD = 7.45). 157 of the participants (< 2%) met criteria for potentially confounding dementias and neurological syndromes (e.g., multiple sclerosis, stroke). Excluding these participants from the sample did not change primary outcome measures ($r_{\text{age correlations (before/after exclusion}}$) > 0.999, mean absolute difference in r = 0.001 for both edges and nodes). Therefore, we retain the full sample for our analyses. Despite previous research demonstrating neuroanatomical sex differences (28,33), we found largely similar patterns of connectome aging across men and women ($r_{\text{edge-age correlations}}$ = 0.892; $r_{\text{node-age correlations}}$ = 0.974, p's < 0.0005). We therefore report results of analyses of data collapsed across both sexes. UKB received ethical approval from the Research Ethics Committee (reference 11/NW/0382). All participants provided informed consent to participate.

Lothian Birth Cohort 1936.—We analyzed data from 534 participants (246 female) from Lothian Birth Cohort 1936 (LBC1936) (34,35) study who had reliable brain MRI and cognitive data at the age-73 wave (mean = 72.8 years; SD = 0.70), the first wave of brain MRI data collection (see Supplementary Materials for full details). Participants in LBC1936 completed an intelligence test at approximately age-11 years as part of the Scottish Mental Survey 1947 (36). Participants were largely healthy: only seven scored in the mild range of

dementia on the Mini-Mental State Exam, zero self-reported symptoms of dementia, and 65 met for neuroradiologically-identified stroke (37).

Brain Image Acquisition and Processing

MRI.—MRI data for UKB participants was collected on the same 3T Siemens Skyra MRI scanner (see Miller et al. (38) & Alfaro-Almagro et al. (39) for full details). MRI data for LBC1936 participants was collected on the same GE Signa Horizon HDx 1.5T clinical scanner (General Electric, Milwaukee, WI) (see Wardlaw et al. (37) for full details). Further details regarding the acquisition and processing of the MRI data can be found in the Supplementary Materials.

Tractography.—Probabilistic tractography pipelines were largely identical across UKB and LBC1936. Details about diffusion tensor MRI (dMRI) acquisition and processing for both samples can be found in the Supplementary Materials.

Connectome Construction.—Treatment of the structural brain data for both samples was based on an automated connectivity mapping pipeline (40,41), wherein T1-weighted volumes are decomposed into 85 distinct cortical and subcortical regions (*nodes*) based on the Desikan-Killiany atlas (42). Mean fractional anisotropy was averaged along the length of all streamlines identified between each pair of nodes (*edges*; $k = 3{,}570$ possible edges). Fractional anisotropy is a dMRI-derived measure of white matter organization that describes the directional coherence of water molecule diffusion. Three edges were estimated as zero across all participants (i.e., probabilistic tractography found no route between the nodes involved). Whole-brain structural connectomes, comprised of the 85 grey matter nodes and the 3,567 non-zero edges, were created for each participant in UKB and LBC1936. Analyses were run using unthresholded matrices, which were determined to be largely similar to consistency-based thresholded matrices (43) (Fig. S1; Supplementary Materials).

Networks-of-Interest.—Masks were created to partition whole-brain connectomes into nine prespecified NOIs (Fig. 1; Table 1; Table S1 & S2). Several NOIs were composed of partially overlapping *edges* and *nodes*, collectively referred to here as *elements* (Table S3). Where applicable, results provide details for how overlapping elements were handled.

Cognitive Testing in LBC 1936

We analyzed data from tests of processing speed, visuospatial ability, and memory, which we have characterized within this cohort in previous research (53). Visuospatial ability was measured using tests of Matrix Reasoning (54), Block Design (54), and Spatial Span (forwards and backwards) (55). Processing speed was measured using the Digit-Symbol Substitution (54), Symbol Search (54), 4-choice reaction time (56), and inspection time (57). Memory was measured using the Digit Span Backward (54), Logical Memory (55), and Verbal Paired Associates (55). All cognitive domains were modeled as latent variables. Fit indices, factor model parameter estimates, and descriptive statistics for the cognitive tests are reported in Table S4.

Results

Connectome Aging

Cross-sectional age trends in each connectome element were estimated in the UKB sample. Density distributions of the element-wise age associations for the whole-brain connectome and each NOI are presented in Fig. 2A. The majority of elements showed small to modest negative associations with age (*edges*: 2,375/3,570 [66.5%] < 0, mean $r = -0.037$, range = −0.437 to 0.268; *nodes*: 81/85 [95.3%] < 0, mean $r = -0.160$, range = −0.322 to 0.087). Nodes from the PFIT network displayed a bimodal distribution of age associations, potentially indicating multiple aging-related processes within this network (Hartigans' dip-test $D = 0.088$, $p < 0.001$; Table S5). This multimodality may be driven by network-specific divisions: elements from the Central Executive network displayed the steepest age-related gradients (mean $r_{\text{age-edge}} = -0.163$; mean $r_{\text{age-node}} = -0.211$; Table S6), suggesting that it demarcates a particularly age-sensitive constellation of elements within the larger PFIT network. Only the Salience network contained a majority of edges with positive age associations (36/45 [80%] r's > 0). In contrast, all ten of its nodes displayed negative age associations.

General dimensions of connectome integrity.—The widespread age-related decrements across NOIs suggests that individual elements may represent broader dimensions of interindividual variation in global connectome integrity. We examined this possibility by residualizing edges and nodes for age and subjecting their respective correlation matrices to principal component analysis (PCA) (Fig. S2 & S3; Tables S7 & S8; Supplementary Materials). The first PC accounted for 11.0% and 36.9% of variation in edges and nodes, respectively. The second PC accounted for less than 1/5 the variance accounted for by the first corresponding Eigen value (Fig. S4). Whole-brain loadings were overwhelmingly positive (*edges*: 98.4% of loadings > 0; *nodes*: 100% of loadings > 0) (Fig. 2B). Elements within the Central Executive network displayed the largest average loadings, potentially driving the bimodal distribution of edges from the PFIT network (Hartigans' dip-test $D = 0.028$, $p = 0.001$; Table S5). This again suggests that this small subset of the PFIT network may disproportionately index overall brain integrity.

Connectome aging occurs along general dimensions of edge and node integrity.—We tested the extent to which aging-related differences in individual connectome elements occurred along the general dimensions of edge and node integrity identified above. In UKB, we estimated the correlation between each element's loading on the first PC (both whole-brain and network-specific) and each element's association with age separately for edges and nodes. Residualizing connectome elements for age prior to conducting PCAs ensured that the tested association between age-sensitivity and PC loadings was *not* an artifact of similar age trends driving element covariation (58,59). Fig. 3 displays the whole-brain association between PC loadings and age correlations for edges (left) and nodes (right). Both edges and nodes that had stronger loadings evinced steeper age-gradients ($r_{\text{edges}} = -0.583$; $r_{\text{nodes}} = -0.420$): the more indicative an element was of global variation in brain connectivity or brain volume, the stronger its negative association

with age. Similar patterns were obtained when analyses were conducted separately for each individual NOI (Figs. S5 & S6; Supplementary Materials).

We tested whether the observed associations between PC loadings and age correlations were explained by the topological centrality (i.e., *strength*) of elements within the whole-brain connectome, a potential indication of metabolic cost that could confer susceptibility to degeneration with age (60) (see Supplementary Materials). We found that topological centrality was strongly correlated with PC loadings (r_{edges} = 0.655; r_{nodes} = 0.583; p's < 0.0005; Fig. S7), but only modestly associated with age correlations (r_{edges} = −0.202, p < 0.0005; r_{nodes} = −0.211, p = 0.053; Fig. S8). Similarly, network membership (i.e., the number of NOIs that an element belongs to) was weakly, if at all, related to the age correlations (Fig. S9). Topological connectedness of connectome elements was therefore insufficient to explain associations between PC loadings and age correlations.

General Dimensions of Connectome Integrity are Associated with Late-Life Cognitive Function

That connectome aging occurs along general dimensions of variation in edge and node integrity suggests that these dimensions may be particularly relevant for cognitive decline. To test this hypothesis, we created linear composite indices of connectome elements in LBC1936 (Fig. S2D), weighted by either UKB-estimated PC loadings or age correlations, to test associations with latent processing speed, visuospatial ability, and memory factors. As would be expected from the sizable associations between age correlations and PC loadings, age-weighted and PC-weighted composites created for the whole brain were highly correlated ($r_{edge\text{-}based\ composites}$ = −0.907; $r_{node\text{-}based\ composites}$ = −0.998) and exhibited nearly-identical patterns of associations with cognitive outcomes. This indicates that brain age and overall integrity are virtually indistinguishable.

Edge-based composites.—Composite indices of connectome-wide edge integrity were significantly associated with processing speed ($r_{age\text{-}weighted}$ = −0.193; 95% CI = [−0.285, −0.101]; $r_{PC\text{-}weighted}$ = 0.177; 95% CI = [0.084, 0.269]), but not with visuospatial ability ($r_{age\text{-}weighted}$ = −0.089; 95% CI = [−0.186, 0.008]; $r_{PC\text{-}weighted}$ = 0.064; 95% CI = [−0.033, 0.162]) or memory ($r_{age\text{-}weighted}$ = −0.083; 95% CI = [−0.186, 0.020]; $r_{PC\text{-}weighted}$ = 0.055; 95% CI = [−0.047, 0.157]). For both age-weights and PC-weights, a 1000-fold permutation test (Fig. S10; Table S9; Supplementary Materials) in which the weights were randomly shuffled across edges indicated that observed edge-based composites were more predictive of both processing speed and visuospatial ability than over 99% of the permuted data (empirical p's < 0.01) and more predictive of memory than over 95% of the permuted data (empirical p's < 0.05).

NOI-based composite indices varied in their magnitudes of prediction of processing speed ($r_{age\text{-}weighted}$ range = −0.193 to −0.037; $r_{PC\text{-}weighted}$ range = −0.095 to 0.186), but displayed null associations with visuospatial ability ($r_{age\text{-}weighted}$ range = −0.130 to 0.009; $r_{PC\text{-}weighted}$ range = −0.064 to 0.100) and memory ($r_{age\text{-}weighted}$ range = −0.099 to −0.003; $r_{PC\text{-}weighted}$ range = −0.030 to 0.100; top left panels of Figs. 4 & S11). To examine whether differences in the magnitudes of association across NOIs stem from differences in their sizes (i.e., larger

networks aggregating more information), we divided each correlation by the total number of elements on which the composite index was based (processing speed: $r_{\text{age-weighted\_adjusted}}$ range = −0.0064 to −0.00005; $r_{\text{PC-weighted\_adjusted}}$ range = −0.0021 to 0.0066; top right panels of Figs. 4 and S11). Edge-based composite indices of Central Executive network integrity showed the largest size-adjusted magnitudes of association with processing speed. As edges were generally unrelated to visuospatial ability and memory, we do not interpret their size-adjusted associations.

Node-based composites.—Composite indices of connectome-wide node integrity were significantly associated with all cognitive domains (processing speed: $r_{\text{age-weighted}} = -0.245$; 95% CI = [−0.335, −0.155]; $r_{\text{PC-weighted}} = 0.234$; 95% CI = [0.145, 0.325]; visuospatial ability: $r_{\text{age-weighted}} = -0.386$; 95% CI = [−0.471, −0.301]; $r_{\text{PC-weighted}} = 0.383$; 95% CI = [0.298, 0.468]; memory: $r_{\text{age-weighted}} = -0.124$; 95% CI = [−0.223, −0.025]; $r_{\text{PC-weighted}} = 0.118$; 95% CI = [0.019, 0.217]). For both age-weights and PC-weights, a 1000-fold permutation test (Fig. S10; Table S9; Supplementary Materials) indicated that observed node-based composites were not substantially more predictive of any domain than the permuted data (empirical p's > 0.09). This is consistent with the high intercorrelations among the nodes, and the observation that the distributions of associations for nearly all permuted node runs were very narrow, indicating that nodes may be largely exchangeable with respect to cognitive ability-relevant information.

NOI-based composite indices varied in their magnitudes of prediction, with prediction of visuospatial ability generally exceeding that of processing speed or memory (processing speed: $r_{\text{age-weighted}}$ range = −0.288 to −0.128; $r_{\text{PC-weighted}}$ range = 0.120 to 0.282; visuospatial ability: $r_{\text{age-weighted}}$ range = −0.377 to −0.277; $r_{\text{PC-weighted}}$ range = 0.292 to 0.373; memory: $r_{\text{age-weighted}}$ range = −0.151 to −0.065; $r_{\text{PC-weighted}}$ range = 0.048 to 0.147; bottom left panels of Figs. 4 & S11). After adjusting for the number of elements, nodes in the Central Executive network displayed the largest associations with all domains of cognitive function (processing speed: $r_{\text{age-weighted\_adjusted}} = -0.026$, 95% CI = [−0.038, −0.015]; $r_{\text{PC-weighted\_adjusted}} = 0.026$, 95% CI = [0.014, 0.037]; visuospatial ability: $r_{\text{age-weighted\_adjusted}} = -0.044$, 95% CI = [−0.055, −0.033]; $r_{\text{PC-weighted\_adjusted}} = 0.044$, 95% CI = [0.033, 0.055]; memory: $r_{\text{age-weighted\_adjusted}} = -0.013$, 95% CI = [−0.025, −0.0003]; $r_{\text{PC-weighted\_adjusted}} = 0.013$, 95% CI = [0.000, 0.025]; bottom right panels of Figs.4 & S11).

General dimensions of edge and node integrity are incrementally predictive of late-life cognitive function.

TBV.: We fitted multiple regression models in LBC1936 to test whether the associations between general dimensions of connectome integrity and cognitive function were unique of TBV, which is perhaps the most robust and well-validated structural MRI predictor of cognitive function (10,14). Results are presented as Model 1 in each panel of Table 2. TBV displayed strong associations with node-based composite scores ($r_{\text{age-weighted}} = -0.869$; $r_{\text{PC-weighted}} = 0.877$; p's < 0.0005), but weak associations with edge-based composites ($r_{\text{age-weighted}} = -0.0004$; $r_{\text{PC-weighted}} = 0.014$; p's > 0.750). TBV was significantly associated with both processing speed ($\beta = 0.165$, $p = 0.001$) and visuospatial ability ($\beta = 0.333$, $p < 0.0005$), but not with memory ($\beta = 0.012$, $p = 0.815$). Edge- and node-based composites of

connectome integrity predicted processing speed incremental of TBV (*edges*: $\beta_{\text{age-weighted}} = -0.194$; $\beta_{\text{PC-weighted}} = 0.176$ *nodes*: $\beta_{\text{age-weighted}} = -0.408$; $\beta_{\text{PC-weighted}} = 0.382$; p's < 0.0005). Node-based composites of connectome integrity predicted visuospatial ability ($\beta_{\text{age-weighted}} = -0.401$; $\beta_{\text{PC-weighted}} = 0.399$; p's < 0.0005) and memory ($\beta_{\text{age-weighted}} = -0.446$; $\beta_{\text{PC-weighted}} = 0.442$; p's < 0.0005) incremental of TBV.

Element type.: We fitted multiple regression models to test whether the associations between edge- and node-based indices of connectome integrity and cognitive function were unique of one another. Results are presented as Model 2 in each panel of Table 2. All associations that were present in the univariate context were preserved. For processing speed, the multiple R^2s from the models that included both edge- and node-based indices were over 40% larger than the R^2s from models including only node-based indices, and over 100% larger than the R^2s from models including only edge-based indices. For visuospatial ability and memory, multiple R^2s from the models that included both edge- and node-based indices were only marginally larger than the R^2s from models including node-based indices alone.

Childhood intelligence.: LBC1936 has available a high-quality index of IQ at age 11 years, the Moray House Test No. 12. Age-11 IQ was associated with node-based indices of age-73 connectome integrity ($\beta_{\text{age-weighted}} = -0.158$; $\beta_{\text{PC-weighted}} = 0.155$; p's < 0.0005), but was not significantly associated with age-73 edge-based indices ($\beta_{\text{age-weighted}} = -0.079$; $\beta_{\text{PC-weighted}} = 0.076$; p's > 0.076). These results are consistent with previous findings in LBC1936 of comparable associations between age-11 IQ and other age-73 structural MRI indices (brain cortical thickness) (61), collectively suggesting that general dimensions of node integrity may at least partially reflect lifelong brain health.

To probe whether associations between age-73 connectome integrity and age-73 cognitive function were plausibly reflective of aging-specific processes, we examined whether the observed associations persisted after controlling for age-11 IQ. Results are presented as Model 3 in each panel of Table 2. Age-73 connectome-integrity indices maintained their associations with age-73 processing speed and visuospatial ability even after controlling for age-11 IQ. The modest node-based associations with memory did not persist after controlling for age-11 IQ.

Regularized LASSO regression models.—We were interested in whether a least absolute shrinkage and selection operator (LASSO) approach for indexing *connectome age* could improve prediction of late-life cognitive function beyond the simple composite indices reported above (see Supplementary Materials for detail). Consistent with previous research that has found differential prediction of age based on brain tissue-type (62), a LASSO model in UKB based on all edges predicted 54.6% of the variance in age in the UKB holdout sample, whereas a model based on all nodes predicted only 35.8% of the variation in age (Fig. S12 & S13; see Supplementary Materials for detail). LASSO-based prediction of cognitive function in LBC1936 from UKB-trained connectome age did not appreciably improve effect sizes relative to estimates obtained using the simple composite indices reported earlier (Fig. S14 & S15), suggesting that the sparsity introduced by complex

algorithmic learning methods is not advantageous for predicting late-life cognitive abilities from connectome aging.

Discussion

Examining variation in elements within the whole-brain structural connectome and several of its NOIs in relation to late-life chronological age and cognitive function may prove fundamental to detecting and mitigating age-related cognitive impairments. Using age-heterogenous data from UKB, we found that connectome age occurs along the same dimensions of global brain health that underlie correlations amongst (age-partialled) connectome element integrities. We used indices of these general dimensions of element integrity in LBC1936 to obtain between-sample cross-validated predictions of aging-sensitive domains of cognitive function in older adulthood (2,63,64). Connectome-wide node integrity was related to all domains of cognitive function, whereas connectome-wide edge integrity was specifically related to processing speed. Associations with processing speed and visuospatial ability persisted after controlling for both TBV and age-11 IQ, suggesting that they capture aging-specific processes. Associations with memory did not survive after controlling for age-11 IQ, suggesting that they may be vestiges of early-life differences in cognitive function. NOI-specific analyses indicated a disproportionally large role of the Central Executive network in these patterns relative to its small size. Edges in the Central Executive network were particularly predictive of processing speed after adjustment, suggesting that the efficacy of water diffusion along white matter pathways between regions such as the dorsolateral prefrontal cortex and the posterior parietal cortex may constrain an individual's ability to efficiently process and act on information.

That connectome elements with stronger loadings on their corresponding PCs had larger negative correlations with age reveals an important connection between individual differences in global neurostructural integrity and aging-related neurodegeneration. This result parallels findings from cognitive aging research that tests with stronger loadings on a general factor of cognitive ability tend to be more closely correlated with age (65,66), suggesting a strong shared basis for cognitive aging across different abilities (67). The current results extend this phenomenon to the brain and highlight that research on individual differences in aging-related cognitive and neurostructural decline would benefit from focusing on broad mechanisms of aging, in addition to more granular processes. This finding also raises considerable interpretation challenges to work on apparent brain age (68,69), suggesting that brain age may index overall connectome health rather than an aging-specific process. Our findings demonstrate that late-life connectome health is partly accounted for by childhood differences in cognitive ability, but that associations between age-73 connectome health and age-73 processing speed and visuospatial ability are also likely to be partly reflective of the aging process proper. Incorporating high-quality controls for prior intelligence or brain structure may facilitate interpreting associations between brain age and external outcomes (70). Not only was connectome age strongly related to connectome integrity, but age-weighted connectome composite scores were nearly entirely collinear with PC-weighted composites ($r_{\text{edge-based composites}} = -0.892$; $r_{\text{node-based composites}} = -0.999$). Thus, any given association with apparent brain age might just as appropriately be conceptualized as an association with overall brain integrity.

Although this study examined a well-characterized set of high-quality structural brain networks in independent, large-scale samples, it nevertheless had some key limitations. First, though the samples were non-overlapping, they were both based in the United Kingdom, self-selected, of the same broad ethnic and cultural background, and healthier, better-educated, and more cognitively able than average (34,35,71). To encourage investigations into the external validity of our findings, we have made the weightings for each of our brain-network predictors publicly available (Table S10). Second, the study focused on neurostructural prediction of cross-sectional differences in cognitive level. Future work might benefit from investigating whether these same predictors are relevant for late-life cognitive change. Research integrating longitudinal measurement of aging-related brain changes with previously-identified determinants of cognitive decline (72), including medical comorbidities, lifestyle indicators, and genetic risk, may critically advance prediction of cognitive aging. Third, though we used unthresholded connectivity matrices, it is possible that edges that occur in few subjects and involve few streamlines contain greater measurement error (73,74). Fourth, the LBC1936 and UKB MRI scanners differed in acquisition strength (1.5T and 3T, respectively). It is potentially nontrivial to compare brain indices across scanners of different magnetic strengths (75,76), and future research would benefit from assessing whether these differences bias cross-sample prediction. Fifth, we used multiple IQ-type tests to model latent variables of three core domains of cognitive function, but it remains unclear how results might generalize to other cognitive domains, such as nonverbal memory (77). Studies using different tests may find somewhat different patterns of relationships between specific brain networks and cognitive abilities. Sixth, previous studies have focused on connectivity *between* several of the networks studied here (78). By primarily investigating networks separately, we may have missed the potential role of between-network connections and cognitive aging. Finally, previous research has examined how aging-related disrupture of *functional* connectivity within specific neural subnetworks relates to cognitive performance in older adults (79,80). Though we focus solely on *structural* connectivity, integrating the structural and functional perspectives is a critical future task for network-focused cognitive neuroscience.

This study represents a comprehensive investigation of aging within the human structural connectome in relation to late-life cognitive function. We found evidence that aging in the brain as a whole, and within specific networks, is related to broad dimensions of variation in neurostructural integrity and is substantially predictive of out-of-sample cognitive abilities. Given the wealth of publicly-available neuroimaging data, the cross-cohort-comparison approach will be fruitful in producing predictively valid estimates of neurostructural associations with cognitive abilities, and thus of potential use in detecting and understanding differences in cognitive decline.

Supplementary Material

Refer to Web version on PubMed Central for supplementary material.

Acknowledgments

This work was supported by National Institutes of Health (NIH) grant R01AG054628. The Population Research Center at the University of Texas is supported by NIH grant P2CHD042849. The Lothian Birth Cohorts group is

funded by Age UK (Disconnected Mind grant), the Medical Research Council (grant MR/R024065/1), and the University of Edinburgh's School of Philosophy, Psychology and Language Sciences. This research was conducted using the UK Biobank Resource (Application Nos. 10279). We thank the UK Biobank participants and UK Biobank team for their work in collecting, processing, and disseminating these data for analysis. A preprint of this paper was posted on *Biorxiv* prior to publication (https://doi.org/10.1101/2019.12.13.875559).

References

1. Park HL, O'Connell JE, Thomson RG (2003): A systematic review of cognitive decline in the general elderly population. Int J Geriatr Psychiatry 18: 1121–1134. [PubMed: 14677145]
2. Tucker-Drob EM (2019): Cognitive Aging and Dementia: A Life-Span Perspective. Annu Rev Dev Psychol 1: 177–196.
3. Jekel K, Damian M, Wattmo C, Hausner L, Bullock R, Connelly PJ, et al. (2015): Mild cognitive impairment and deficits in instrumental activities of daily living: a systematic review. Alzheimers Res Ther 7: 17. [PubMed: 25815063]
4. Tucker-Drob EM (2011): Neurocognitive functions and everyday functions change together in old age. Neuropsychology 25: 368–377. [PubMed: 21417532]
5. Comas-Herrera A, Wittenberg R, Pickard L, Knapp M (2007): Cognitive impairment in older people: future demand for long-term care services and the associated costs. Int J Geriatr Psychiatry 22: 1037–1045. [PubMed: 17603823]
6. Fjell AM, Walhovd KB (2010): Structural brain changes in aging: courses, causes and cognitive consequences. Rev Neurosci 21: 187–221. [PubMed: 20879692]
7. Cox SR, Ritchie SJ, Tucker-Drob EM, Liewald DC, Hagenaars SP, Davies G, et al. (2016): Ageing and brain white matter structure in 3,513 UK Biobank participants. Nat Commun 7: 13629. [PubMed: 27976682]
8. Fjell AM, McEvoy L, Holland D, Dale AM, Walhovd KB (2014): What is normal in normal aging? Effects of aging, amyloid and Alzheimer's disease on the cerebral cortex and the hippocampus. Prog Neurobiol 117: 20–40. [PubMed: 24548606]
9. Pietschnig J, Penke L, Wicherts JM, Zeiler M, Voracek M (2015): Meta-analysis of associations between human brain volume and intelligence differences: How strong are they and what do they mean? Neurosci Biobehav Rev 57: 411–432. [PubMed: 26449760]
10. Gignac GE, Bates TC (2017): Brain volume and intelligence: The moderating role of intelligence measurement quality. Intelligence 64: 18–29.
11. Haász J, Westlye ET, Fjær S, Espeseth T, Lundervold A, Lundervold AJ (2013): General fluid-type intelligence is related to indices of white matter structure in middle-aged and old adults. NeuroImage 83: 372–383. [PubMed: 23791837]
12. Kochunov P, Williamson DE, Lancaster J, Fox P, Cornell J, Blangero J, Glahn DC (2012): Fractional anisotropy of water diffusion in cerebral white matter across the lifespan. Neurobiol Aging 33: 9–20. [PubMed: 20122755]
13. Penke L, Maniega SM, Bastin ME, Valdés Hernández MC, Murray C, Royle NA, et al. (2012): Brain white matter tract integrity as a neural foundation for general intelligence. Mol Psychiatry 17: 1026–1030. [PubMed: 22614288]
14. Cox SR, Ritchie SJ, Fawns-Ritchie C, Tucker-Drob EM, Deary IJ (2019): Structural brain imaging correlates of general intelligence in UK Biobank. Intelligence 76: 101376. [PubMed: 31787788]
15. Yarkoni T, Westfall J (2017): Choosing Prediction Over Explanation in Psychology: Lessons From Machine Learning. Perspect Psychol Sci 12: 1100–1122. [PubMed: 28841086]
16. Poldrack RA, Huckins G, Varoquaux G (2019): Establishment of Best Practices for Evidence for Prediction: A Review. JAMA Psychiatry. 10.1001/jamapsychiatry.2019.3671
17. Sporns O (2011): The human connectome: a complex network. Ann N Y Acad Sci 1224: 109–125. [PubMed: 21251014]
18. Fox MD, Snyder AZ, Vincent JL, Corbetta M, Van Essen DC, Raichle ME (2005): From The Cover: The human brain is intrinsically organized into dynamic, anticorrelated functional networks. Proc Natl Acad Sci 102: 9673–9678. [PubMed: 15976020]

19. Dosenbach NUF, Fair DA, Miezin FM, Cohen AL, Wenger KK, Dosenbach RAT, et al. (2007): Distinct brain networks for adaptive and stable task control in humans. Proc Natl Acad Sci U S A 104: 11073–11078. [PubMed: 17576922]
20. Catani M, Dell'acqua F, Thiebaut de Schotten M (2013): A revised limbic system model for memory, emotion and behaviour. Neurosci Biobehav Rev 37: 1724–1737. [PubMed: 23850593]
21. Rolls ET (2015): Limbic systems for emotion and for memory, but no single limbic system. Cortex J Devoted Study Nerv Syst Behav 62: 119–157.
22. Alexander GE, DeLong MR, Strick PL (1986): Parallel organization of functionally segregated circuits linking basal ganglia and cortex. Annu Rev Neurosci 9: 357–381. [PubMed: 3085570]
23. Wang D, Buckner RL, Fox MD, Holt DJ, Holmes AJ, Stoecklein S, et al. (2015): Parcellating cortical functional networks in individuals. Nat Neurosci 18: 1853–1860. [PubMed: 26551545]
24. Menon V (2015): Salience Network. Brain Mapping. Elsevier, pp 597–611.
25. Ham T, Leff A, de Boissezon X, Joffe A, Sharp DJ (2013): Cognitive control and the salience network: an investigation of error processing and effective connectivity. J Neurosci Off J Soc Neurosci 33: 7091–7098.
26. Jung RE, Haier RJ (2007): The Parieto-Frontal Integration Theory (P-FIT) of intelligence: converging neuroimaging evidence. Behav Brain Sci 30: 135–154; discussion 154–187. [PubMed: 17655784]
27. Basten U, Hilger K, Fiebach CJ (2015): Where smart brains are different: A quantitative meta-analysis of functional and structural brain imaging studies on intelligence. Intelligence 51: 10–27.
28. Gong G, Rosa-Neto P, Carbonell F, Chen ZJ, He Y, Evans AC (2009): Age- and Gender-Related Differences in the Cortical Anatomical Network. J Neurosci 29: 15684–15693. [PubMed: 20016083]
29. Zhao T, Cao M, Niu H, Zuo X-N, Evans A, He Y, et al. (2015): Age-related changes in the topological organization of the white matter structural connectome across the human lifespan. Hum Brain Mapp 36: 3777–3792. [PubMed: 26173024]
30. Zhao L, Matloff W, Ning K, Kim H, Dinov ID, Toga AW (2019): Age-Related Differences in Brain Morphology and the Modifiers in Middle-Aged and Older Adults. Cereb Cortex N Y N 1991 29: 4169–4193.
31. Smith SM, Elliott LT, Alfaro-Almagro F, McCarthy P, Nichols TE, Douaud G, Miller KL (2020): Brain aging comprises many modes of structural and functional change with distinct genetic and biophysical associations. eLife 9: e52677. [PubMed: 32134384]
32. Sudlow C, Gallacher J, Allen N, Beral V, Burton P, Danesh J, et al. (2015): UK biobank: an open access resource for identifying the causes of a wide range of complex diseases of middle and old age. PLoS Med 12: e1001779. [PubMed: 25826379]
33. Ritchie SJ, Cox SR, Shen X, Lombardo MV, Reus LM, Alloza C, et al. (2018): Sex Differences in the Adult Human Brain: Evidence from 5216 UK Biobank Participants. Cereb Cortex 28: 2959–2975. [PubMed: 29771288]
34. Deary IJ, Gow AJ, Pattie A, Starr JM (2012): Cohort profile: the Lothian Birth Cohorts of 1921 and 1936. Int J Epidemiol 41: 1576–1584. [PubMed: 22253310]
35. Taylor AM, Pattie A, Deary IJ (2018): Cohort Profile Update: The Lothian Birth Cohorts of 1921 and 1936. Int J Epidemiol 47: 1042–1042r. [PubMed: 29546429]
36. Scottish Council for Research in Education (Ed.) (1933): The Intelligence of Scottish Children. University of London Press.
37. Wardlaw JM, Bastin ME, Valdés Hernández MC, Maniega SM, Royle NA, Morris Z, et al. (2011): Brain aging, cognition in youth and old age and vascular disease in the Lothian Birth Cohort 1936: rationale, design and methodology of the imaging protocol. Int J Stroke Off J Int Stroke Soc 6: 547–559.
38. Miller KL, Alfaro-Almagro F, Bangerter NK, Thomas DL, Yacoub E, Xu J, et al. (2016): Multimodal population brain imaging in the UK Biobank prospective epidemiological study. Nat Neurosci 19: 1523–1536. [PubMed: 27643430]
39. Alfaro-Almagro F, Jenkinson M, Bangerter NK, Andersson JLR, Griffanti L, Douaud G, et al. (2018): Image processing and Quality Control for the first 10,000 brain imaging datasets from UK Biobank. NeuroImage 166: 400–424. [PubMed: 29079522]

40. Buchanan CR, Pernet CR, Gorgolewski KJ, Storkey AJ, Bastin ME (2014): Test–retest reliability of structural brain networks from diffusion MRI. NeuroImage 86: 231–243. [PubMed: 24096127]
41. Buchanan CR, Pettit LD, Storkey AJ, Abrahams S, Bastin ME (2015): Reduced structural connectivity within a prefrontal-motor-subcortical network in amyotrophic lateral sclerosis. J Magn Reson Imaging JMRI 41: 1342–1352. [PubMed: 25044733]
42. Desikan RS, Ségonne F, Fischl B, Quinn BT, Dickerson BC, Blacker D, et al. (2006): An automated labeling system for subdividing the human cerebral cortex on MRI scans into gyral based regions of interest. NeuroImage 31: 968–980. [PubMed: 16530430]
43. Buchanan CR, Bastin ME, Ritchie SJ, Liewald DC, Madole JW, Tucker-Drob EM, et al. (2020): The effect of network thresholding and weighting on structural brain networks in the UK Biobank. NeuroImage 211: 116443. [PubMed: 31927129]
44. Sridharan D, Levitin DJ, Menon V (2008): A critical role for the right fronto-insular cortex in switching between central-executive and default-mode networks. Proc Natl Acad Sci U S A 105: 12569–12574. [PubMed: 18723676]
45. Menon V, Uddin LQ (2010): Saliency, switching, attention and control: a network model of insula function. Brain Struct Funct 214: 655–667. [PubMed: 20512370]
46. Fair DA, Dosenbach NUF, Church JA, Cohen AL, Brahmbhatt S, Miezin FM, et al. (2007): Development of distinct control networks through segregation and integration. Proc Natl Acad Sci U S A 104: 13507–13512. [PubMed: 17679691]
47. Duncan J (2010): The multiple-demand (MD) system of the primate brain: mental programs for intelligent behaviour. Trends Cogn Sci 14: 172–179. [PubMed: 20171926]
48. Fedorenko E, Duncan J, Kanwisher N (2013): Broad domain generality in focal regions of frontal and parietal cortex. Proc Natl Acad Sci 110: 16616–16621. [PubMed: 24062451]
49. Bressler SL, Menon V (2010): Large-scale brain networks in cognition: emerging methods and principles. Trends Cogn Sci 14: 277–290. [PubMed: 20493761]
50. Aggleton JP (2008): EPS Mid-Career Award 2006: Understanding anterograde amnesia: Disconnections and hidden lesions. Q J Exp Psychol 61: 1441–1471.
51. Vann SD, Aggleton JP, Maguire EA (2009): What does the retrosplenial cortex do? Nat Rev Neurosci 10: 792–802. [PubMed: 19812579]
52. Yeo BT, Krienen FM, Sepulcre J, Sabuncu MR, Lashkari D, Hollinshead M, et al. (2011): The organization of the human cerebral cortex estimated by intrinsic functional connectivity. J Neurophysiol 106: 1125–1165. [PubMed: 21653723]
53. Ritchie SJ, Tucker-Drob EM, Cox SR, Corley J, Dykiert D, Redmond P, et al. (2016): Predictors of ageing-related decline across multiple cognitive functions. Intelligence 59: 115–126. [PubMed: 27932854]
54. Wechsler David (1998): Wechsler Adult Intelligence Scale III-UK Administration and Scoring Manual. Psychological Corporation.
55. Wechsler David (1998): Wechsler Memory Scale III-UK Administration and Scoring Manual. Psychological Corporation.
56. Deary I (2001): Reaction times and intelligence differences A population-based cohort study. Intelligence 29: 389–399.
57. Deary IJ, Simonotto E, Meyer M, Marshall A, Marshall I, Goddard N, Wardlaw JM (2004): The functional anatomy of inspection time: an event-related fMRI study. NeuroImage 22: 1466–1479. [PubMed: 15275904]
58. Lindenberger U, von Oertzen T, Ghisletta P, Hertzog C (2011): Cross-sectional age variance extraction: What's change got to do with it? Psychol Aging 26: 34–47. [PubMed: 21417539]
59. Hofer SM, Sliwinski MJ (2001): Understanding Ageing. Gerontology 47: 341–352. [PubMed: 11721149]
60. Perry A, Wen W, Lord A, Thalamuthu A, Roberts G, Mitchell PB, et al. (2015): The organisation of the elderly connectome. NeuroImage 114: 414–426. [PubMed: 25869857]
61. Karama S, Bastin ME, Murray C, Royle NA, Penke L, Muñoz Maniega S, et al. (2014): Childhood cognitive ability accounts for associations between cognitive ability and brain cortical thickness in old age. Mol Psychiatry 19: 555–559. [PubMed: 23732878]

62. Richard G, Kolskår K, Sanders A-M, Kaufmann T, Petersen A, Doan NT, et al. (2018): Assessing distinct patterns of cognitive aging using tissue-specific brain age prediction based on diffusion tensor imaging and brain morphometry. PeerJ 6: e5908. [PubMed: 30533290]
63. Salthouse TA (1996): The processing-speed theory of adult age differences in cognition. Psychol Rev 103: 403–428. [PubMed: 8759042]
64. Tucker-Drob EM (2011): Global and domain-specific changes in cognition throughout adulthood. Dev Psychol 47: 331–343. [PubMed: 21244145]
65. Salthouse TA (2001): Structural models of the relations between age and measures of cognitive functioning. Intelligence 29: 93–115.
66. Salthouse TA (2004): From Description to Explanation in Cognitive Aging. In: Sternberg RJ, Pretz JE, editors. Cognition and Intelligence. Cambridge: Cambridge University Press, pp 288–305.
67. Tucker-Drob EM, Brandmaier AM, Lindenberger U (2019): Coupled cognitive changes in adulthood: A meta-analysis. Psychol Bull 145: 273–301. [PubMed: 30676035]
68. Cole JH, Marioni RE, Harris SE, Deary IJ (2019): Brain age and other bodily 'ages': implications for neuropsychiatry. Mol Psychiatry 24: 266–281. [PubMed: 29892055]
69. Kaufmann T, van der Meer D, Doan NT, Schwarz E, Lund MJ, Agartz I, et al. (2019): Common brain disorders are associated with heritable patterns of apparent aging of the brain. Nat Neurosci 22: 1617–1623. [PubMed: 31551603]
70. Elliott ML, Belsky DW, Knodt AR, Ireland D, Melzer TR, Poulton R, et al. (2019): Brain-age in midlife is associated with accelerated biological aging and cognitive decline in a longitudinal birth cohort. Mol Psychiatry. 10.1038/s41380-019-0626-7
71. Fry A, Littlejohns TJ, Sudlow C, Doherty N, Adamska L, Sprosen T, et al. (2017): Comparison of Sociodemographic and Health-Related Characteristics of UK Biobank Participants With Those of the General Population. Am J Epidemiol 186: 1026–1034. [PubMed: 28641372]
72. Corley J, Cox SR, Deary IJ (2018): Healthy cognitive ageing in the Lothian Birth Cohort studies: marginal gains not magic bullet. Psychol Med 48: 187–207. [PubMed: 28595670]
73. Roberts JA, Perry A, Roberts G, Mitchell PB, Breakspear M (2017): Consistency-based thresholding of the human connectome. NeuroImage 145: 118–129. [PubMed: 27666386]
74. Betzel RF, Griffa A, Hagmann P, Mišić B (2019): Distance-dependent consensus thresholds for generating group-representative structural brain networks. Netw Neurosci Camb Mass 3: 475–496.
75. Jovicich J, Czanner S, Han X, Salat D, van der Kouwe A, Quinn B, et al. (2009): MRI-derived measurements of human subcortical, ventricular and intracranial brain volumes: Reliability effects of scan sessions, acquisition sequences, data analyses, scanner upgrade, scanner vendors and field strengths. NeuroImage 46: 177–192. [PubMed: 19233293]
76. Chen J, Liu J, Calhoun VD, Arias-Vasquez A, Zwiers MP, Gupta CN, et al. (2014): Exploration of scanning effects in multi-site structural MRI studies. J Neurosci Methods 230: 37–50. [PubMed: 24785589]
77. Drag LL, Bieliauskas LA (2010): Contemporary Review 2009: Cognitive Aging. J Geriatr Psychiatry Neurol 23: 75–93. [PubMed: 20101069]
78. Chand GB, Wu J, Hajjar I, Qiu D (2017): Interactions of the Salience Network and Its Subsystems with the Default-Mode and the Central-Executive Networks in Normal Aging and Mild Cognitive Impairment. Brain Connect 7: 401–412. [PubMed: 28707959]
79. Geerligs L, Maurits NM, Renken RJ, Lorist MM (2014): Reduced specificity of functional connectivity in the aging brain during task performance: Functional Connectivity in the Aging Brain. Hum Brain Mapp 35: 319–330. [PubMed: 22915491]
80. Geerligs L, Renken RJ, Saliasi E, Maurits NM, Lorist MM (2015): A Brain-Wide Study of Age-Related Changes in Functional Connectivity. Cereb Cortex 25: 1987–1999. [PubMed: 24532319]

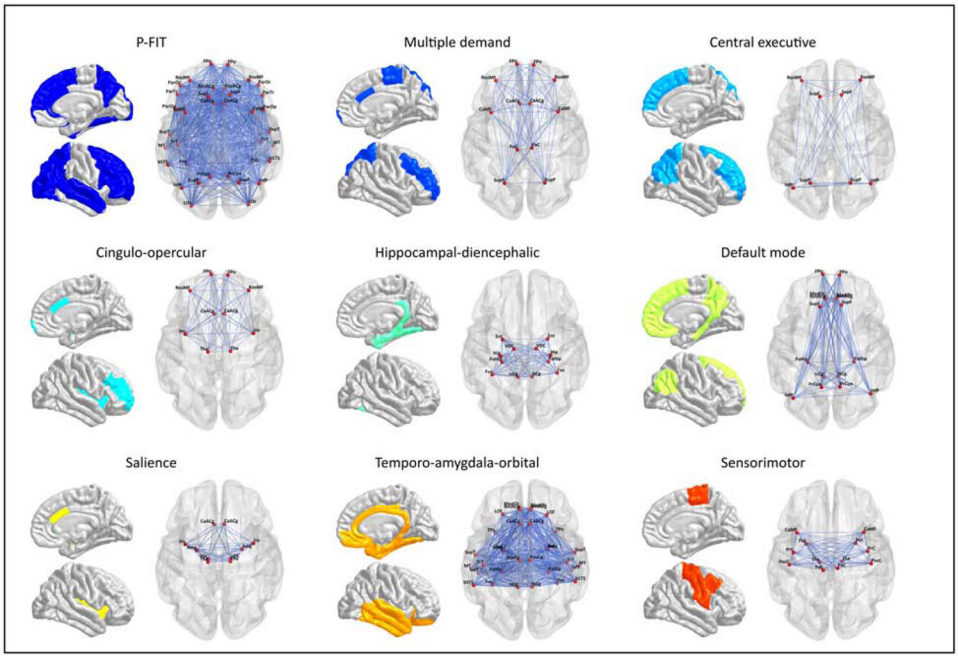

Figure 1. Anatomical maps of each NOI.

Anatomical maps of each prespecified brain NOI displaying the network-specific connectome elements (*i.e.*, edges and nodes).

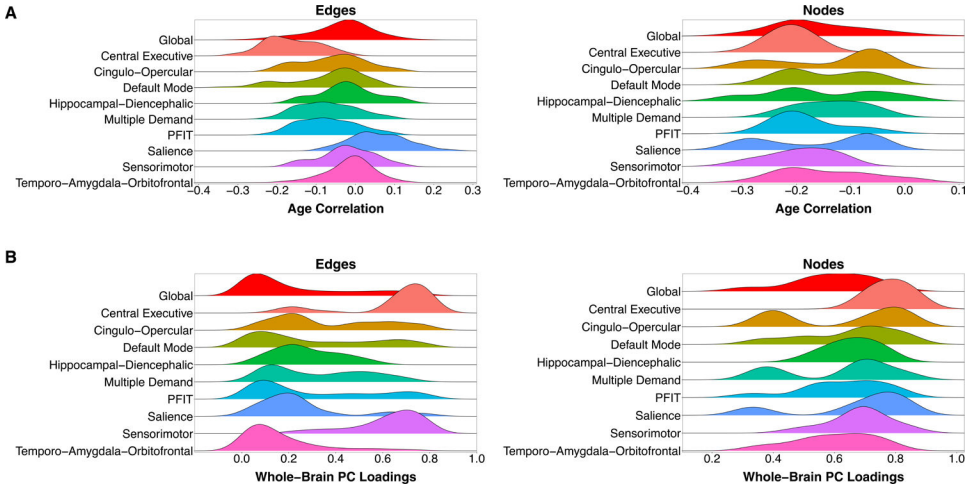

Figure 2. Density distributions of age associations and whole-brain principal component loadings.

A) Density distributions of each element's association with age, categorized by prespecified NOI. All NOIs are subsets of the whole-brain (Global) network, such that comparison with the red distribution at the top of both panels is not a comparison of independent elements, but a comparison of a subset to a whole. **B)** Density distributions of loadings on the first principal component of the whole-brain connectome, categorized by prespecified NOI. Principal component analyses were conducted separately for each NOI.

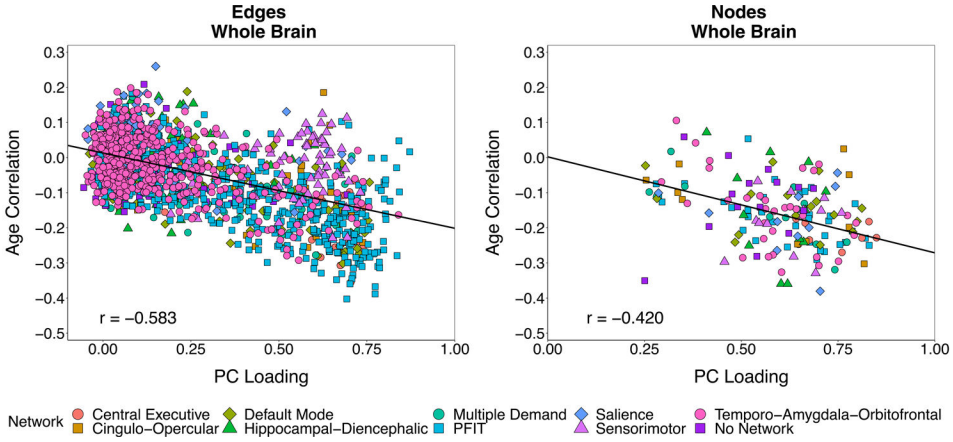

Figure 3. Scatterplot of age correlations and principal component loadings.

Scatterplots of each connectome element's correlation with age against its loading on a single principal component (based on an age-partialled correlation matrix (Fig. S2)). Analyses were conducted separately for edges (left) and nodes (right). Each point represents a single element of the connectome (3,567 non-zero edges; 85 nodes). Points are categorized by the NOI to which the element belongs. Elements belonging to multiple NOIs are plotted once for each group membership and jittered for the sake of visual interpretation. Reported correlations and displayed regression lines reflect analyses including each element only once.

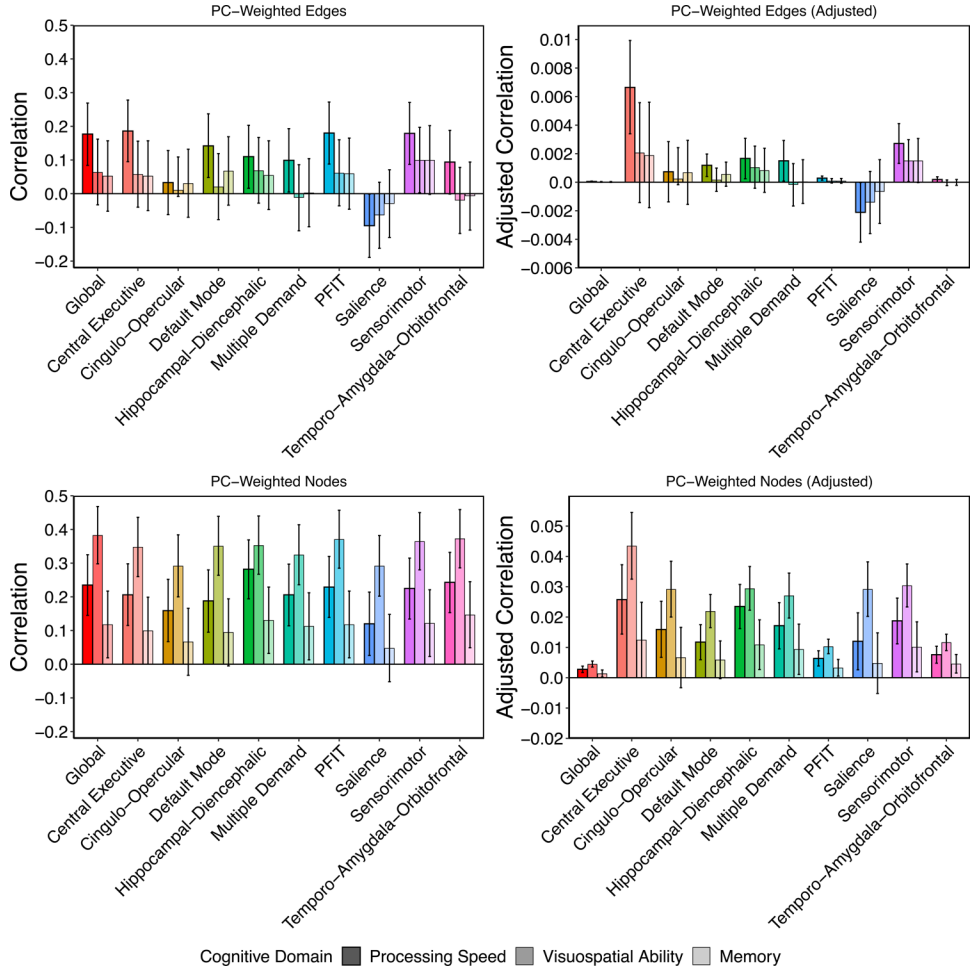

Figure 4. Prediction of cognitive function in LBC1936 from UKB-weighted indices of connectome integrity.

Raw and adjusted associations between weighted-composite scores reflecting variation in overall connectome integrity and cognitive function in LBC1936. Adjusted estimates were created by dividing the raw estimates by the number of edges or nodes in the network. Note that raw associations for edges and nodes are presented on the same *y*-axis scale, whereas the scale for the adjusted associations differs for edges and nodes. Scores were created across the whole brain and all NOIs by summing the LBC1936 data weighted by each element's loading on the first principal component of its respective subnetwork discovered in UK Biobank. Plots are broken down by element type (*i.e.*, edges or nodes) and reflect correlations between respective weighted composites from each NOI and the cognitive domains of processing speed, visuospatial ability, and memory. Error bars represent 95% confidence intervals.

Table 1.

Properties of each brain NOI, with a canonical reference describing the network's makeup, previous associations and elements.

Network	Number of Nodes	Number of Edges	Hypothesis	Select Regions	Implicated in
All networks (global)	85	3570	+		
PFIT (26, 27)	36	630	+	DLPFC, inferior and superior parietal lobule, anterior cingulate, and specific regions within the temporal and occipital lobes	General intelligence
Central Executive (44–46)	8	28	+	rDLPFC, posterior parietal cortex	Activation associated with selecting, switching, and attending to salient events
Multiple Demand (47,48)	12	66	+	middle frontal, inferior parietal, pre-SMA, anterior cingulate, rostral prefrontal, insula/frontal operculum	General purpose activation in cognitive demanding tasks, suggesting a role in cognitive flexibility, executive control, and abstract problem solving
Cingulo-Opercular (46)	10	45	+	dorsal anterior cingulate, superior and anterior frontal cortex, insula, thalamus	Stable set control, maintenance of task-relevant sustained attention
Default Mode (20,49)	16	120	−	ventromedial frontal, medial temporal and posterior cingulate cortices, angular gyrus and cingulum bundle	Extensive de-activation in functional MRI during cognitively demanding tasks
Hippocampal-Diencephalic (50,51)	12	66	+	hippocampus, diencephalon, ventral cingulum and fornix	Memory and spatial orientation
Salience (24,25,45)	10	45	−	insula, anterior cingulate cortex, amygdala, substantia nigra/VTA and thalamus	Orientation of attention to the most homeostatically relevant even from moment to moment
Sensorimotor (22,23)	12	66	−	precentral, postcentral, pre and post SMA, caudal cingulate, caudal middle frontal, thalamus, putamen	Initiation and control of movements
Temporo-Amygdala-Orbital (20,21)	32	496	−	anterior temporal cortex, amygdala and orbitofrontal cortices, ACC, and parts of cingulum bundle	Visceral emotion and sensation

Note. For each network, the number of edges is N*((N-1)/2) the number of nodes. + refers to subnetwork for which we hypothesized a positive association between subnetwork integrity and cognitive function. – refers to a negative control network, i.e. a network for which we do not hypothesize a positive association between subnetwork integrity and cognitive function. See Fig. 1 for illustration of network properties. See Table S2 for comparison to other widely-used brain subnetworks (52).

Biol Psychiatry. Author manuscript; available in PMC 2022 April 15.

Table 2.

Associations between weighted connectome (edge and node) composites, total brain volume, and age-11 IQ.

Table 2a: Processing Speed							
Composite	***Model***	***Predictor 1***	***Predictor 2***	***β1* (*p*-value)**	***β2* (*p*-value)**	***R*²**	***Multiple R***
Age-based	1a	-	TBV	-	0.165 (0.001)	0.027	0.165
	1b	Edges	TBV	−0.194 (< 0.0005)	0.165 (< 0.0005)	0.065	0.255
	1c	Nodes	TBV	−0.408 (< 0.0005)	−0.188 (0.049)	0.069	0.263
	2a	Edges only	-	−0.193 (< 0.0005)	-	0.037	0.193
	2b	-	Nodes only	-	−0.245 (< 0.0005)	0.060	0.245
	2c	Edges	Nodes	−0.167 (< 0.0005)	−0.226 (< 0.0005)	0.088	0.297
	3a	-	Age 11 IQ	-	0.511 (< 0.0005)	0.261	0.511
	3b	Edges	Age 11 IQ	−0.149 (0.001)	0.498 (< 0.0005)	0.282	0.531
	3c	Nodes	Age 11 IQ	−0.162 (< 0.0005)	0.484 (< 0.0005)	0.285	0.535
PC-based	4a	-	TBV	-	0.165 (0.001)	0.027	0.165
	4b	Edges	TBV	0.176 (< 0.0005)	0.163 (0.001)	0.058	0.241
	4c	Nodes	TBV	0.382 (< 0.0005)	−0.168 (0.089)	0.062	0.249
	5a	Edges only	-	0.177 (< 0.0005)	-	0.031	0.177
	5b	-	Nodes only	-	0.235 (< 0.0005)	0.055	0.235
	5c	Edges	Nodes	0.154 (0.001)	0.219 (< 0.0005)	0.079	0.281
	6a	-	Age 11 IQ	-	0.511 (< 0.0005)	0.261	0.511
	6b	Edges	Age 11 IQ	0.133 (0.002)	0.500 (< 0.0005)	0.277	0.526
	6c	Nodes	Age 11 IQ	0.154 (< 0.0005)	0.486 (< 0.0005)	0.283	0.532
Table 2b: Visuospatial Ability							
Composite	*Model*	*Predictor 1*	*Predictor 2*	*β1* (*p*-value)	*β2* (*p*-value)	*R*²	*Multiple R*
Age-based	1a	-	TBV	-	0.333 (< 0.0005)	0.111	0.333
	1b	Edges	TBV	−0.087 (0.068)	0.331 (< 0.0005)	0.117	0.342
	1c	Nodes	TBV	−0.401 (< 0.0005)	−0.017 (0.860)	0.149	0.386
	2a	Edges only	-	−0.089 (0.072)	-	0.008	0.089
	2b	-	Nodes only	-	−0.386 (< 0.0005)	0.149	0.386
	2c	Edges	Nodes	−0.043 (0.363)	−0.380 (< 0.0005)	0.150	0.387
	3a	-	Age 11 IQ	-	0.553 (< 0.0005)	0.306	0.553
	3b	Edges	Age 11 IQ	−0.039 (0.387)	0.549 (< 0.0005)	0.307	0.554
	3c	Nodes	Age 11 IQ	−0.308 (< 0.0005)	0.504 (< 0.0005)	0.397	0.630
PC-based	4a	-	TBV	-	0.333 (< 0.0005)	0.111	0.333
	4b	Edges	TBV	0.058 (0.224)	0.331 (< 0.0005)	0.114	0.338

Table 2a: Processing Speed							
Composite	***Model***	***Predictor 1***	***Predictor 2***	***β1* (*p*-value)**	***β2* (*p*-value)**	***R*^{2}**	***Multiple R***
	4c	Nodes	TBV	0.399 (< 0.0005)	−0.019 (0.848)	0.147	0.383
	5a	Edges only	-	0.064 (0.197)	-	0.004	0.064
	5b	-	Nodes only	-	0.383 (< 0.0005)	0.147	0.383
	5c	Edges	Nodes	0.023 (0.633)	0.380 (< 0.0005)	0.147	0.383
	6a	-	Age 11 IQ	-	0.553 (< 0.0005)	0.306	0.553
	6b	Edges	Age 11 IQ	0.017 (0.702)	0.552 (< 0.0005)	0.306	0.553
	6c	Nodes	Age 11 IQ	0.306 (< 0.0005)	0.505 (< 0.0005)	0.397	0.630

Table 2c: Memory							
Composite	*Model*	*Predictor 1*	*Predictor 2*	*β1* (*p*-value)	*β2* (*p*-value)	*R*^{2}	*Multiple R*
Age-based	1a	-	TBV	-	0.012 (0.815)	0.0001	0.012
	1b	Edges	TBV	−0.082 (0.117)	0.009 (0.861)	0.007	0.084
	1c	Nodes	TBV	−0.446 (< 0.0005)	−0.370 (< 0.0005)	0.049	0.221
	2a	Edges only	-	−0.083 (0.116)	-	0.007	0.083
	2b	-	Nodes only	-	−0.124 (0.014)	0.015	0.124
	2c	Edges	Nodes	−0.067 (0.204)	−0.166 (0.023)	0.020	0.141
	3a	-	Age 11 IQ	-	0.613 (< 0.0005)	0.376	0.613
	3b	Edges	Age 11 IQ	−0.027 (0.557)	0.615 (< 0.0005)	0.381	0.617
	3c	Nodes	Age 11 IQ	−0.033 (0.468)	0.611 (< 0.0005)	0.381	0.617
PC-based	4a	-	TBV	-	0.012 (0.815)	0.0001	0.012
	4b	Edges	TBV	0.052 (0.329)	0.009 (0.863)	0.003	0.055
	4c	Nodes	TBV	0.442 (< 0.0005)	−0.369 (< 0.0005)	0.045	0.214
	5a	Edges only	-	0.053 (0.324)	-	0.003	0.053
	5b	-	Nodes only	-	0.118 (0.019)	0.014	0.118
	5c	Edges	Nodes	0.037 (0.483)	0.114 (0.026)	0.015	0.122
	6a	-	Age 11 IQ	-	0.613 (< 0.0005)	0.376	0.613
	6b	Edges	Age 11 IQ	−0.003 (0.954)	0.616 (< 0.0005)	0.379	0.616
	6c	Nodes	Age 11 IQ	0.029 (0.524)	0.612 (< 0.0005)	0.380	0.616

Note. TBV = Total brain volume.

KEY RESOURCES TABLE

Resource Type	Specific Reagent or Resource	Source or Reference	Identifiers	Additional Information
Add additional rows as needed for each resource type	Include species and sex when applicable.	Include name of manufacturer, company, repository, individual, or research lab. Include PMID or DOI for references; use “this paper” if new.	Include catalog numbers, stock numbers, database IDs or accession numbers, and/or RRIDs. RRIDs are highly encouraged; search for RRIDs at https://scicrunch.org/resources.	Include any additional information or notes if necessary.
Biological Sample	In vivo human brain volume	UK Biobank	RRID:SCR_012815	
Biological Sample	In vivo human white matter connectivity	UK Biobank	RRID:SCR_012815	
Biological Sample	In vivo human brain volume	Lothian Birth Cohort 1936		https://www.lothianbirthcohort.ed.ac.uk
Biological Sample	In vivo human white matter connectivity	Lothian Birth Cohort 1936		https://www.lothianbirthcohort.ed.ac.uk
Deposited Data; Public Database	UK Biobank	UK Biobank	RRID:SCR_012815	
Software; Algorithm	R project for statistical computing	http://www.r-project.org/	RRID:SCR_001905	
Software; Algorithm	R: *ggplot2* package	ttps://cran.r-project.org/web/packages/ggplot2/index.html	RRID:SCR_014601	
Software; Algorithm	R: *lavaan* package	doi: 10.18637/jss.v048.i02		
Software; Algorithm	R: *cv.glmnet* package	https://pubmed.ncbi.nlm.nih.gov/20808728/		
Software; Algorithm	R: *caret* package	https://github.com/topepo/caret/		
Software; Algorithm	R: *igraph* package	http://igraph.org		
Software; Algorithm	Freesurfer	http://surfer.nmr.mgh.harvard.edu/	RRID:SCR_001847	
Software; Algorithm	FSL	http://www.fmrib.ox.ac.uk/fsl	RRID:SCR_002823	
Software; Algorithm	BEDPOSTx	http://www.fmrib.ox.ac.uk/fsl	RRID:SCR_002823	
Software; Algorithm	PROBTRACKx	http://www.fmrib.ox.ac.uk/fsl	RRID:SCR_002823	
Software; Algorithm	BrainNet Viewer	http://www.nitrc.org/projects/bnv/	RRID:SCR_009446	

Biol Psychiatry. Author manuscript; available in PMC 2022 April 15.